International Journal for Modern Trends in Science and Technology, 9(04): 20-30, 2023

ISSN: 2455-3778 online
DOI: https://doi.org/10.46501/IJMTST0904004
Available online at: http://www.ijmtst.com/vol9issue04.html

A Generic Model to Analyze and Predict Brain Tumor from MRI and CT Medical Images using Deep Learning

Dr. D.Sirisha | A Anusha | V Sridevi | SSL Kalyan | T Naga Vikas Reddy

Department of Information Technology, Pragati Engineering College (A), Surampalem (East Godavari) A.P,India.

To Cite this Article
Dr. D.Sirisha, A Anusha, V Sridevi, SSL Kalyan and T Naga Vikas Reddy. A Generic Model to Analyze and Predict Brain Tumor from MRI and CT Medical Images using Deep Learning. International Journal for Modern Trends in Science and Technology 2023, 9(04), pp. 20-30. https://doi.org/10.46501/IJMTST0903004

Article Info
Received: 02 March 2023; Accepted: 25 March 2023; Published: 30 March 2023.

ABSTRACT

Deep neural networks are now the state-of-the-art machine learning models across a variety of areas, from image analysis to natural language processing, and considerably posted in academia. These developments have a huge eventuality for medical imaging technology, medical data analysis, medical diagnostics and healthcare in general, sluggishly being realized. A short overview of recent advances and some associated challenges in machine literacy applied to medical image processing and image analysis are provided in this paper. This paper focuses on deep literacy in MRI. The tremendous success of machine literacy algorithms at image recognition tasks in recent times intersects with a time of dramatically increased use of electron medical records and individual imaging. This review introduces the machine learning algorithms applied to medical image analysis, fastening on convolutional neural networks, and emphasizing clinical aspects of the field. The advantage of machine literacy in medical big data is that a significant Hierarchal connections within the data can be discovered algorithmically without laborious hand-casting of features. Moreover, Crucial exploration areas and operations of medical image bracket, localization, discovery, segmentation, and enrollment are emphasized and the paper concludes by agitating exploration obstacles, arising trends, and possible unborn directions.

KEYWORDS – Convolutional neural networks, medical image analysis, machine learning, deep learning.

1. INTRODUCTION

Machine learning has seen some dramatic developments recently, leading to a lot of interest from industry, academia user-friendly software frameworks, and an explosion of the available compute power, enabling the use of neural networks that are deeper than ever before [27]. These models nowadays form popular culture. These are driven by breakthroughs in the state-of-the-art approach to a wide variety of problems in artificial neural networks, often termed deep learning, a set of techniques and algorithms that enable computers to discover complicated patterns in large data sets. Feeding the breakthroughs is the increased access to data ("big data"), computer vision, language modeling and robotics. Deep learning rose to its prominent position in computer vision when neural networks started outperforming other methods on several high-profile image analysis benchmarks. Most famously on the ImageNet Large-Scale Visual Recognition Challenge (ILSVRC) in 2012 when a deep learning model (a convolutional neural network) halved the second-best error rate on the image classification task. Enabling

computers to recognize objects in natural images was until recently thought to be a very difficult task, but by now convolutional neural networks have surpassed even human performance on the ILSVRC, and reached a level where the ILSVRC classification task is essentially solved (i.e., with error rate close to the Bayes rate). Deep learning techniques have become the de facto standard for a wide variety of computer vision problems. They are, however, not limited to image processing and analysis but are outperforming other approaches in areas like natural language processing, speech recognition and synthesis and in the analysis of unstructured, tabular-type data using entity embeddings. The sudden progress and wide scope of deep learning, and the resulting surge of attention and multi-billion-dollar investment, has led to a virtuous cycle of improvements and investments in the entire field of machine learning [28]. It is now one of the hottest areas of study world-wide, and people with competence in machine learning are highly sought-after by both industry and academia. Healthcare providers generate and capture enormous amounts of data containing extremely valuable signals and information, at a pace far surpassing what "traditional" methods of analysis can process. Machine learning therefore quickly enters the picture, as it is one of the best ways to integrate, analyze and make predictions based on large, heterogeneous data sets (cf. health informatics). Healthcare applications of deep learning range from one-dimensional bio signal analysis and the prediction of medical events, e.g. seizures and cardiac arrests, to computer-aided detection and diagnosis supporting clinical decision making and survival analysis , to drug discovery and as an aid in therapy selection and pharmacogenomics , to increased operational efficiency, stratified care delivery, and analysis of electronic health records. Machine learning algorithms have the potential to be invested deeply in all fields of medicine, from drug discovery to clinical decision making, significantly altering the way medicine is practiced. The success of machine learning algorithms at computer vision tasks in recent years comes at an opportune time when medical records are increasingly digitalized [30]. The use of electronic health records (EHR) quadrupled from 11.8% to 39.6% amongst office-based physicians in the US from 2007 to 2012. Medical images are an integral part of a patient's EHR and are currently analyzed by human radiologists, who are limited by speed, fatigue, and experience. It takes years and great financial cost to train a qualified radiologist, and some health-care systems outsource radiology reporting to lower-cost countries such as India via tele-radiology. A delayed or erroneous diagnosis cause harm to the patient. Therefore, it is ideal for medical image analysis to be carried out by an automated, accurate and efficient machine learning algorithm. Medical image analysis is an active field of research for machine learning, partly because the data is relatively structured and labelled, and it is likely that this will be the area where patients first interact with functioning, practical artificial intelligence systems. This is significant for two reasons. Firstly, in terms of actual patient metrics, medical image analysis is a litmus test as to whether artificial. The aim of the work presented in this paper is to develop and test a Deep Learning approach for brain tumor classification and segmentation using a Multiscale Convolutional Neural Network. To train and test the proposed neural model, a T1-CE MRI image dataset from 233 patients, including meningiomas, gliomas, and pituitary tumors in the common views (sagittal, coronal, and axial), has been used. Figure 1 shows examples of these three types of tumors. Additional information on the dataset is included in Section 2.2. The proposed model is able to segment and predict the pathological type of the three kinds of brain tumors, outperforming previous studies using the same dataset.

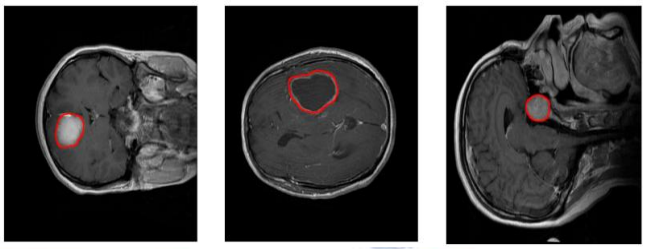

Figure 1. Examples of MRI images of the T1-CE MRI image dataset. Left: coronal view of a meningioma tumor. Center: Axial view of a glioma tumor. Right: sagittal view of a pituitary tumor. Tumor borders have been highlighted in red.

In the BTS field, two main tumor segmentation approaches can be found: generative and discriminative. Generative approaches use explicit anatomical models to obtain the segmentation, while discriminative methods learn image features and their relations using gold standard expert segmentations. Published studies

following the discriminative approach have evolved from using classical Machine Learning to more recent Deep Learning techniques.

2. Preliminaries and Related Work

In this section, firstly, we propose a multi-pathway CNN, for tumor segmentation. The CNN architecture processes an MRI image (slice) pixel by pixel covering the entire image and classifying each pixel using one of four possible outputs

2.1. Machine learning, artificial neural networks, deep learning

In machine learning one develops and studies methods that give computers the ability to solve problems by learning from experiences. The goal is to create mathematical models that can be trained to produce useful outputs when fed input data. Machine learning models are provided experiences in the form of training data, and are tuned to produce accurate predictions for the training data by an optimization algorithm. The main goal of the models are to be able to generalize their learned expertise, and deliver correct predictions for new, unseen data. A model's generalization ability is typically estimated during training using a separate data set, the validation set, and used as feedback for further tuning of the model. After several iterations of training and tuning, the final model is evaluated on a test set, used to simulate how the model will perform when faced with new, unseen data. There are several kinds of machine learning, loosely categorized according to how the models utilize its input data during training. In reinforcement teaching one constructs agents that learn from their environments through trial and error while optimizing some objective function. A famous recent application of reinforcement learning is AlphaGo and AlphaZero, the Go-playing machine learning systems developed by DeepMind. In unsupervised learning the computer is tasked with uncovering patterns in the data without our guidance. Clustering is a prime example. Most of today's machine learning systems belong to the class of supervised learning. Here, the computer is given a set of already labeled or annotated data, and asked to produce correct labels on new, previously unseen data sets based on the rules discovered in the labeled data set. From a set of input-output examples, the whole model is trained to perform specific data-processing tasks. Image annotation using human-labeled data, e.g. classifying skin lesions according to malignancy or discovering cardiovascular risk factors from retinal fundus photographs, are two examples of the multitude of medical imaging related problems attacked using supervised learning. Machine learning has a long history and is split into many sub-fields, of which deep learning is the one currently receiving the bulk of attention. There are many excellent, openly available overviews and surveys of deep learning. For short general introductions to deep learning, see. For an in-depth coverage, consult the freely available book. For a broad overview of deep learning applied to medical imaging, Only some bare essentials of the field, hoping that will serve as useful pointers to the areas that are currently the most influential in medical imaging are specified.

2.2. Proposed Convolutional Neural Network and Implementation Details

In this paper, we propose a multi-pathway CNN architecture (see Figure 2) for tumor segmentation. The CNN architecture processes an MRI image (slice) pixel by pixel covering the entire image and classifying each pixel using one of four possible output labels: 0—healthy region, 1—meningioma tumor, 2—glioma tumor, and 3—pituitary tumor. In our approach, we use a sliding window, thus each pixel is classified according to a N * N neighborhood or window, which is the input to our CNN architecture (see Figure2). Every window is processed through three convolutional pathways with three scale (large, medium, and small) kernels that extract the features. In our implementation, we chose a window of 65 * 65 pixels and kernels of size 11 * 11, 7 * 7 and 3 * 3 pixels, respectively.

The decision on the size of the windows was taken after preliminary configuration tests in which also 33 * 33 px and 75 * 75 px window sizes were tested. Each pathway is composed by two convolutional stages with ReLU rectification and 3 * 3 max-pooling kernels with a stride value of 2. The number of feature maps in the large, medium, and small pathways is 128, 96, and 64, respectively. We propose the use of a larger number of maps for larger scales with the assumption that the window features extracted using different filtering scales help to define the three kinds of tumor to be classified. Scale features from the three pathways are concatenated in a convolutional layer with 3 * 3 kernels with a ReLU

activation function and a 2 * 2 max-pooling kernel with a stride value of 2. The output of this stage enters a fully connected stage where 8192 concatenated scale features compose the classification method towards the four prediction label types. In order to prevent overfitting, the model includes a dropout layer before the fully connected layer. The last layer uses a SoftMax activation function. The proposed CNN has been implemented using Pytorch™. The number of trainable parameters in the neural network is near three million (2,856,932). All the tests have been performed in a Linux environment with an Intel Core i5 CPU and an Nvidia GTX1080 T1-11GB GPU. The training process took 5 days, and the average prediction time per image was 57.5 s.

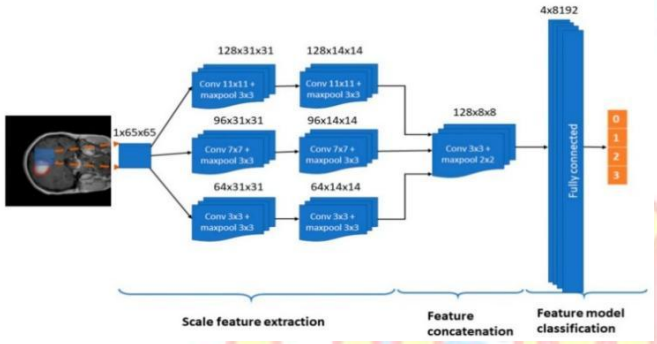

Figure 2. The proposed Convolutional Neural Networks (CNN) architecture. Input: 1 X 65 X 65 sliding windows. Model: Three pathways (large, medium, and small feature scales) with 2 convolutional layers and max-pooling, a convolutional layer with concatenation of the three pathways, and a fully connected stage that leads to a classification in one out of the four possible output labels: 0—healthy region, 1—meningioma tumor, 2—glioma tumor, and 3—pituitary tumor. A dropout mechanism between the concatenation and fully connected stages is included.

2.3. Building blocks of convolutional neural networks

When applying neural networks to images one can in principle use the simple feedforward neural networks discussed above. However, having connections from all nodes of one layer to all nodes in the next is extremely inefficient. A careful pruning of the connections based on domain knowledge, i.e. the structure of images, leads to much better performance. A CNN is a particular kind of artificial neural network aimed at preserving spatial relationships in the data, with very few connections between the layers. The input to a CNN is arranged in a grid structure and then fed through layers that preserve these relationships, each layer operation operating on a small region of the previous layer (Fig. 2). CNNs are able to form highly efficient representation of the input data, well-suited for image-oriented tasks. A CNN has multiple layers of convolutions and activations, often interspersed with pooling layers, and is trained using backpropagation and gradient descent as for standard artificial neural networks. In addition, CNNs typically have fully connected layers at the end, which compute the final outputs. (i) Convolutional layers: In the convolutional layers the activations from the previous layers are convolved with a set of small parameterized filters, frequently of size 3 × 3, collected in a tensor W (j,i) , where j is the filter number and i is the layer number. By having each filter share the exact same weights across the whole input domain, i.e. translational equivariance at each layer, one achieves a drastic reduction in the number of weights that need to be learned. The motivation for this weight-sharing is that features appearing in one part of the image likely also appear in other parts. If you have a filter capable of detecting horizontal lines, say, then it can be used to detect them wherever they appear. Applying all the convolutional filters at all locations of the input to a convolutional layer produces a tensor of feature maps.

(ii) Activation layer: The feature maps from a convo approximate almost any nonlinear function. The activation functions are generally the very simple rectified linear units, or ReLUs, defined as ReLU(z) = max(0, z), or variants like leaky ReLUs or parametric ReLUs. Feeding the feature maps through an activation function produces new tensors, typically also called feature maps. (iii) Pooling: Each feature map produced by feeding the data through one or more convolutional layer is then typically pooled in a pooling layer. Pooling operations take small grid regions as input and produce single numbers for each region. The number is usually computed by using the max function (max-pooling) or the average function (average pooling). Since a small shift of the input image results in small changes in the activation maps, the pooling layers gives the CNN some translational invariance. A different way of getting the down sampling effect of pooling is to use convolutions with increased stride lengths. Removing the pooling layers simplifies the network architecture without necessarily sacrificing performance. Other common

elements in many modern CNNs include (iv) Dropout regularization: A simple idea that gave a huge boost in the performance of CNNs. By averaging several models in an ensemble, one tends to get better performance than when using single models. Dropout is an averaging technique based on stochastic sampling of neural networks. By randomly removing neurons during training, one ends up using slightly different networks for each batch of training data, and the weights of the trained network are tuned based on optimization of multiple variations of the network. (v) Batch normalization: These layers are typically placed after activation layers, producing normalized activation maps by subtracting the mean and dividing by the standard deviation for each training batch. Including batch normalization layers forces the network to periodically change its activations to zero mean and unit standard deviation as the training batch hits these layers, which works as a regularized for the network, speeds up training, and makes it less dependent on careful parameter initialization [66].

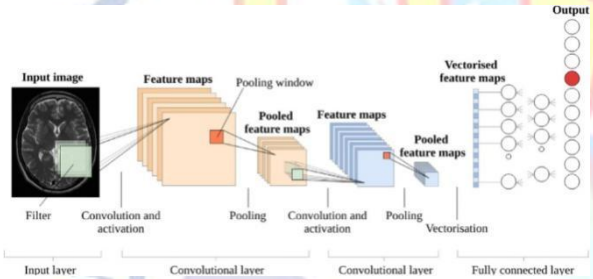

Figure 3. Building blocks of a typical CNN. A slight modification of a figure in [58], courtesy of the author.

In the design of new and improved CNN architectures, these components are combined in increasingly complicated and interconnected ways, or even replaced by other more convenient operations. When architecting a CNN for a particular task there are multiple factors to consider, including understanding the task to be solved and the requirements to be met, figuring out how to best feed the data to the network, and optimally utilizing one's budget for computation and memory consumption. In the early days of modern deep learning, one tended to use very simple combinations of the building blocks, as in Lenet and AlexNet. Later network architectures are much more complex, each generation building on ideas and insights from previous architectures, resulting in updates to the state-of-the-art. Table 1 contains a short list of some famous CNN architectures, illustrating how the building blocks can be combined and how the field moves along. These neural networks are typically implemented in one or more of a small number of software frameworks that dominates machine learning research, all built on top of NVIDIA's CUDA platform and the cuDNN library. Today's deep learning methods are almost exclusively implemented in either TensorFlow, a framework originating from Google Research, Keras, a deep learning library originally built by Fran¸cois Chollet and recently incorporated in TensorFlow, or Pytorch, a framework associated with Facebook Research. There are very few exceptions (YOLO built using the Darknet framework is one of the rare ones). All the main frameworks are open source and under active development.

3. SYSTEM FRAMEWORK

To the researcher, CNNs have been put to task for classification, localization, detection, segmentation and registration in image analysis. Machine learning research draws a distinction between localization (draw a bounding box around a single object in the image), and detection (draw bounding boxes around multiple objects, which may be from different classes). Segmentation draws outlines around the edges of target objects, and labels them (semantic segmentation). Registration refers to fitting one image (which may be 2 or 3 dimensional) onto another. This separation of tasks is based on different machine learning techniques and is maintained below. To the clinician this separation of tasks is not that crucial, and it is the authors' opinion that a pragmatic machine learning system will incorporate some or all of the tasks into a unified system. It would be ideal to, in a single workflow, detect a lung tumor on a CT chest scan, and then localize and segment it away from normal tissue, and to prognosticate various treatment options, such as chemotherapy or surgery. Indeed, some of these task's blur into one another in the papers discussed here. From the clinician's perspective, classification ascertains if a disease state is present or not, i.e., is blood present on this MRI brain scan signifying a hemorrhagic stroke? Localization implies the identification of normal anatomy, for example, where is the kidney in this ultrasound image? This is in contrast to detection,

which implies an abnormal, pathological state, for example, all the lung tumors in the CT scan of the lung can be identified by segmenting the outline of a lung tumor that helps the clinician to determine its distance from major anatomical structures, and helps to answer a question such as, should this patient be operated on, and if so, what should be the extent of resection.

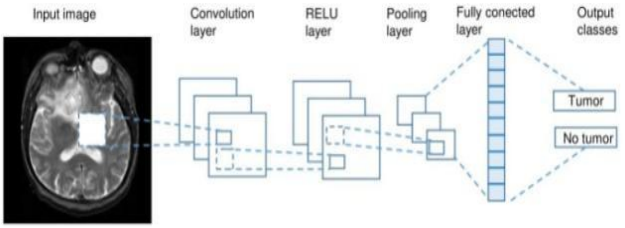

FIGURE 4. In this example disease classification task, an input image of an abnormal axial slice of a T2-weighted MRI brain is run through a schematic depiction of a CNN. Feature extraction of the input image is performed via the Convolution, RELU and pooling layers, before classification by the fully connected layer.

3.1 CLASSIFICATION

Classification is sometimes also known as Computer-Aided Diagnosis (CADx). Lo et al. described a CNN to detect lung nodules on chest X-rays as far back as 1995. They used 55 chest x-rays and a CNN with 2 hidden layers to output. whether or not a region had a lung nodule. The relative availability of chest x-ray images has likely accelerated deep learning progress in this modality. Rajkomar et al. augmented 1850 chest x-ray images into 150,000 training samples. Using a modified pre-trained GoogLeNet CNN, they classified the orientation of the images into frontal or lateral views with near 100% accuracy. Although this task of identifying the orientation of the chest x-ray is of limited clinical use, it does demonstrate the effectiveness of pre-training, and data augmentation in learning the relevant image metadata, as part of an eventually fully-automated diagnostic workflow. Pneumonia or chest infection is a common health-problem world-wide that is eminently treatable. Rajpurkar et al. employed a modified DenseNet with 121 convolutional layers called CheXNet to classify 14 different diseases seen on the chest x-rays, using 112,000 images from the ChestXray14 dataset. CheXNet achieved state of the art performance in classifying the 14 diseases; pneumonia classification in particular achieved an Area Under Curve (AUC) score of 0.7632 with Receiver Operating Characteristics (ROC) analysis. Moreover, on a test set of 420 images, CheXNet matched or bettered the performance of 4 individual radiologists, and also the performance of a panel comprising of 3 radiologists. Shen et al. used CNNs combined with Support Vector Machine (SVM) and Random Forest (RF) classifiers to classify lung nodules into benign or malignant, based on 1010 labelled CT lung scans from the Lung Image Database Consortium (LIDC-IDRI) dataset. They used 3 parallel CNNs with 2 convolution layers each, with each CNN taking image patches at different scales to extract features. The learned features were used to construct an output feature vector, which was then classified using either a SVM with radial basis function (RBF) filter or RF classifier into benign or malignant.

Their method classified nodules with 86% accuracy and they also found that it was robust against different levels of noise inputs. Li et al. used 3-dimensional CNNs to interpolate missing imaging data between MRI and PET images.

830 patients with MRI and PET scans from the Alzheimer Disease Neuroimaging Initiative (ADNI) database were studied. 3-D CNNs were trained with MRI and PET images as input and output respectively, and used to reconstruct PET images from patients who did not have them. Their reconstructed PET images almost matched ground truth results of disease classification, but one caveat is that issues of overfitting were not addressed, limiting the potential generalizability of their technique. Hosseini-Asl et al. achieved state of the art results in diagnosing patients with Alzheimer's Disease versus normal, with an accuracy of 99%. They employed 3-D CNNs in an autoencoder architecture, pretrained on the CADDementia dataset to learn generic brain structural features. The learned feature outputs were then connected to higher layers where deep supervision techniques fine-tuned the algorithm's ability to discriminate between scans of patients with normal brains, mild cognitive impairment, or Alzheimer's Disease from the ADNI database. Korolev et al. evaluated the performance of their VOXCNN and ResNet, which was based on the VGGNet and Residual neural network architectures respectively. They also used the ADNI database to discriminate between normal

and Alzheimer Disease patients. Although their accuracy of 79% for Voxnet and 80% for ResNet was lower than what Hosseini-Asl achieved, Korolev states that their algorithms did not need hand-crafting of features and were simpler to implement. Diabetic retinopathy (DR) can also be diagnosed using CNNs. Using digital photographs of the fundus of the eye, Pratt et al. trained a CNN with 10 convolutional layers and 3 fully connected layers on approximately 90,000 fundus images. They classified DR into 5 clinically used classifications of DR severity, with 75% accuracy. Abramoff et al. evaluated a commercial device, the IDx-DR version X2.1 (IDx LLC, Iowa City, Iowa, USA) to detect DR. The author does not disclose the CNN architectures but states they are inspired by Alexnet and VGGNet. The device, trained on up to 1.2 million DR images, obtained an AUC score of 0.98. Unsupervised learning methods are also an active area of research. Plis et al. used Deep Belief Networks to extract features from functional fMRI (fMRI) images, and MRI scans of patients with Huntington Disease and Schizophrenia. Suk et al. classified fMRI images into diagnoses of Healthy or Mild Cognitive Impairment, using a stacked architecture of RBMs to learn hierarchal functional relationships between different brain regions. Looking outside the usual CNN models, Kumar et al. compared the performance of the well-known CNNs Alexnet and VGGNet to other techniques, namely Bag of Visual Words (BOVV) and Local Binary Patterns (LBP). Interestingly, the BOVV technique performed the best at classifying histopathological images into 20 different tissue types.

3.2 LOCALIZATION

Localization of normal anatomy is less likely to interest the practicing clinician although applications may arise in anatomy education. Alternatively, localization may find use in fully automated end-to-end applications, whereby the radiological image is autonomously analyzed and reported without any human intervention. Yan et al. looked at transverse CT image slices and constructed a two stage CNN where the first stage identified local patches, and the second stage discriminated the local patches by various body organs, achieving better results than a standard CNN. Roth et al. trained a CNN with 5 convolution layers to discriminate approximately 4000 transverse axial CT images into one of 5 categories: neck, lung, liver, pelvis, legs. He was able to achieve a 5.9% classification error rate and an AUC score of 0.998, after data augmentation techniques. Shin et al. used stacked autoencoders on 78 contrast-enhanced MRI scans of the abdominal region containing liver or kidney metastatic tumors, to detect the locations of the liver, heart, kidney and spleen. Hierarchal features were learned over the spatial and temporal domains, giving detection accuracies of between 62% and 79%, depending on the organ.

3.3 DETECTION

Detection, sometimes known as Computer-Aided Detection (CADe) is a keen area of study as missing a lesion on a scan can have drastic consequences for both the patient and the clinician. The task for the Kaggle Data Science Bowl of 2017 involved the detection of cancerous lung nodules on CT lung scans. Approximately 2000 CT scans were released for the competition and the winner Fangzhou achieved a logarithmic loss score of 0.399. Their solution used a 3-D CNN inspired by U-Net architecture to isolate local patches first for nodule detection. Then this output was fed into a second stage consisting of 2 fully connected layers for classification of cancer probability. Shin et al. evaluated five well-known CNN architectures in detecting thoracoabdominal lymph nodes and Interstitial lung disease on CT scans. Detecting lymph nodes is important as they can be a marker of infection or cancer. They achieved a mediastinal lymph node detection AUC score of 0.95 with a sensitivity of 85% using GoogLeNet, which was state of the art. They also documented the benets of transfer learning, and the use of deep learning architectures of up to 22 layers, as opposed to fewer layers which was the norm in medical image analysis. Overfeat was a CNN pre-trained on natural images that won the ILSVRC 2013 localization task . Ciompi et al. applied Overfeat to 2-dimensional slices of CT lung scans oriented in the coronal, axial and sagittal planes, to predict the presence of nodules within and around lung pressures. They combined this approach with simple SVM and RF binary classifiers, as well as a Bag of Frequencies, a novel 3-dimensional descriptor of their own invention.

3.4 SEGMENTATION

CT and MRI mage segmentation research covers a variety of organs such as liver, prostate and knee cartilage, but a large amount of work has focused on brain segmentation, including tumor segmentation. The latter is especially important in surgical planning to determine the exact boundaries of the tumor in order to direct surgical resection. Sacrificing too much of eloquent brain areas during surgery would cause neurological deficits such as limb weakness, numbness and cognitive impairment. Traditionally, medical anatomical segmentation was done by hand, with a clinician drawing out- lines slice by slice through an entire MRI or CT volume stack, therefore it is ideal to implement a solution that automates this laborious task. An excellent review of brain MRI segmentation was written by Akkus et al., who reviewed various CNN architectures and metrics used in segmentation. Additionally, he also detailed the numerous competitions and their datasets, such as Brain Tumor Segmentation (BRATS), Mild traumatic brain injury outcome prediction (MTOP) and Ischemic Stroke Lesion Segmentation (ISLES). Moeskops et al. used 3 CNNs, each with a different 2-dimensional input patch size, running in parallel to classify and segment MRI brain images of 22 pre-term infants and 35 adults into different tissue classes such as white matter, grey matter and cerebrospinal fluid. The advantage of using 3 different input patch sizes is that each focuses on capturing different aspects of the image, with the smallest patch focused on local textures while the larger patch sizes assimilated spatial features. Overall, the algorithm achieved good accuracy,

3.5 REGISTRATION

Although the registration of medical images has many potential applications, which were reviewed by El-Gamal et al. their actual clinical use is encountered in niche areas. Image registration is employed in neurosurgery or spinal surgery, to localize a tumor or spinal bony landmark, in order to facilitate surgical tumor removal or spinal screw implant placement. A reference image is aligned to a second image, called a sense image and various similarity measures and reference points are calculated to align the images, which can be 2 or 3-dimensional. The reference image may be. a pre-operative MRI brain scan and the sense image may be an intraoperative MRI brain scan done after a first-pass resection, to determine if there is remnant tumor and if further resection is required. Using MRI brain scans from the OASIS dataset, Yang et al. stacked convolution layers in an encoder-decoder fashion, to predict how an input pixel would morph into its final configuration. They invoked the use of a large deformation diffeomorphic metric mapping (LDDMM) registration model and achieved dramatic improvements in computational time. Miao et al. trained a 5-layer CNN on synthetic X-ray images in order to register 3-dimensional models of a knee implant, a hand implant, and a trans-esophageal probe onto 2-dimensional X-ray images, in order to estimate their pose. Their method obtained successful registrations 79-99% of the time, and took 0.1 seconds, a significant improvement over traditional intensity-based registration method.

4. EVALUATION

4.0. Comparison with other Methods

Segmentation performance metrics of our method (see Table1) are in the range of the wining proposals in the well-known brain tumor image segmentation challenge BRATS. This benchmark uses glioma tumor images and supplies a dataset with four modalities of MRI (T1, T2, T1-CE, and FLAIR). The 2013 top-ten ranking of the participating methods obtained glioma Dice index values between 0.69 and 0.82 for the segmentation of the complete tumor. The Dice index value obtained by our method for glioma segmentation is 0.779, which is close to the highest achieved value, even with the inconveniences associated with working with a single MRI modality and classifying among three different kinds of tumors. A more appropriate comparison of our results is with those results obtained by previous works using the same T1-CE MRI image dataset. Table4shows the tumor classification accuracy of our approach, together with seven published methods: two feature-driven approaches and five deep learning approaches. Our method outperforms the other proposals with a tumor classification accuracy of 0.973.

Table 1. Comparison of the proposed approach with other approaches over the same T1-CE MRI image dataset.

Authors	Classification Method	Tumor Classification Accuracy
Cheng et al. [5]	SVM	0.912
Cheng et al. [32]	Fisher kernel	0.947
Abiwinanda et al. [24]	CNN	0.841
Pashaei et al. [25]	CNN	0.810
Pashaei et al. [25]	CNN and KELM	0.936
Sultan et al. [26]	CNN	0.961
Anaraki et al. [27]	CNN and GA	0.942
Our approach	Multiscale CNN	0.973

4.3.1. Evaluation of tumor classification

The classification function, depends on the confidence threshold parameter below fig. shows the relationship between the confidence threshold and the resulting precision. A slow descent can be observed up to a confidence threshold of 0.88 followed by a sharp decline. There is no strong restriction on the selection of the confidence threshold and, in order to obtain a classification with a precision level higher than 0.9, it could be the behavior could be predicted observing the pttas index histogram. Peak values in the histogram can be found once a pttas value of 0.88 is reached. The number of images with a pttas index value between 0.4 and 0.88 is very low, so when the confidence threshold is raised from 0.4 to 0.88, the precision will only be marginally lower as can be observed in the graph in Figure5. Due to the fact that all the processed images with a pttas index value greater than 0.4 are correctly labeled, if we were to choose a confidence threshold equal or lower than 0.4, the precision would be close to 100% (all samples would be correctly labeled, except those with a value close to zero). This is why the confidence threshold diagram begins with accuracy ~1 (= 0.994).

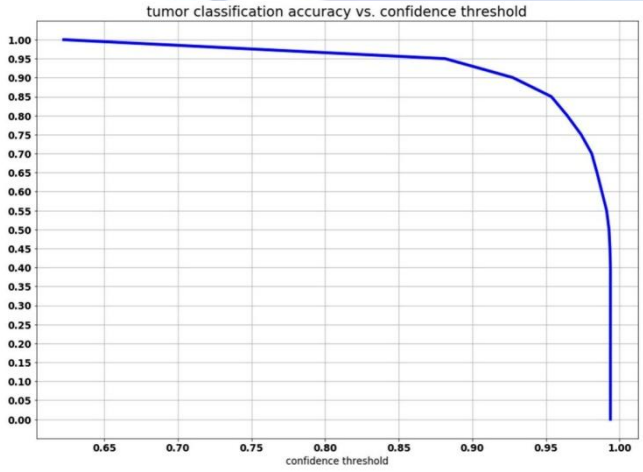

Figure 5. Graph of the relation between the confidence threshold and the precision of the predicted tumor type.

5. CONCLUSION

In this paper, we present a fully automatic brain tumor segmentation and classification method, based on a CNN architecture designed for multiscale processing. We evaluated its performance using a publicly available T1-weighted contrast-enhanced MRI images dataset. Data augmentation through elastic transformation was adopted to increase the training dataset and prevent overfitting. The measures of performance obtained are in the range of the top ten methods from the BRATS 2013 benchmark. We compared our results with other seven brain tumor classification approaches that used the same dataset. Our method obtained the highest tumor classification accuracy with a value of 0.973. Our multiscale CNN approach, which uses three processing pathways, is able to successfully segment and classify the three kinds of brain tumors in the dataset: meningioma, glioma, and pituitary tumor. In spite of the fact that skull and vertebral column parts are not removed and the variability of the three tumor types, which caused false positives in some images, our approach achieved outstanding segmentation performance metrics, with an average Dice index of 0.828, an average Sensitivity of 0.940, and an average pttas value of 0.967. Our method can be used to assist medical doctors in the diagnostics of brain tumors and the proposed segmentation and classification method can be applied to other medical imaging problems. As future work, we plan to develop an FCN architecture for the classification of the same MRI images dataset and compare its performance with the proposed model. Moreover, we plan to study the applicability of the proposed multiscale convolutional neural network for segmentation in other research fields such as satellite imagery.

Conflict of interest statement

Authors declare that they do not have any conflict of interest.

REFERENCES

[1] Mohan, G.; Subashin, M. MRI based medical image analysis: Survey on brain tumor grade classification. Biomed. Signal Process. Control 2018, 39, 139–161. [CrossRef]

[2] I¸sın, A.; Direko˘glu, C.; ¸Sah, M. Review of MRI-based brain tumor image segmentation using deep learning methods. Procedia Comput. Sci. 2016, 102, 317–324. [CrossRef]

[3] Menze, B.J.; Jakab, A.; Bauer, S.; Kalpathy-Cramer, J.; Farahani, K.; Kirby, J.; Burren, Y.; Porz, N.; Slotboom, J.; Wiest, R.; et al. The multimodal brain tumor image segmentation benchmark (BRATS). IEEE Trans. Med. Imaging 2015, 34, 1993–2024. [CrossRef] [PubMed]

[4] Litjens, G.; Kooi, T.; Bejnordi, B.E.; Arindra, A.; Setio, A.; Ciompi, F.; Ghafoorian, M.; van der Laak, J.A.W.M.; van Ginneken, B.; Sánchez, C.I. A survey on deep learning in medical image analysis. Med. Image Anal. 2017, 42, 60–88. [CrossRef] [PubMed]

[5] Cheng, J.; Huang, W.; Cao, S.; Yang, R.; Yang, W.; Yun, Z.; Wang, Z.; Feng, Q. Enhanced performance of brain tumor classification via tumor region augmentation and partition. PLoS ONE 2015, 10, e0140381.

[6] Sachdeva, J.; Kumar, V.; Gupta, I.; Khandelwal, N.; Ahuja, C.K. A package-SFERCB-"Segmentation, features extraction, reduction and classification analysis by both SVM and ANN for brain tumors". Appl. Soft Comput. 2016, 47, 151–167. [CrossRef]

[7] Sharma, Y.; Chhabra, M. An improved automatic brain tumor detection system. Int. J. Adv. Res. Comput. Sci. Softw. Eng. 2015, 5, 11–15.

[8] Iftekharuddin, K.M.; Zheng, J.; Islam, M.A.; Ogg, R.J. Fractal-based brain tumor detection in multimodal MRI. Appl. Math. Comput. 2009, 207, 23–41. [CrossRef]

[9] Havaei, M.; Jodoin, P.-M.; Larochelle, H. Efficient Interactive Brain Tumor Segmentation as Within-Brain kNN Classification. In Proceedings of the 22nd International Conference on Pattern Recognition, Stockholm, Sweden, 24–28 August 2014; IEEE: Los Alamitos, CA, USA, 2014; pp. 556–561.

[10] Havaei, M.; Davy, A.; Warde-Farley, D.; Biard, A.; Courville, A.; Bengio, Y.; Pal, C.; Jodoin, P.-M.; Larochelle, H. Brain tumor segmentation with deep neural networks. Med. Image Anal. 2017, 35, 18–31. [CrossRef]

[11] Moeskops, P.; de Bresser, J.; Kuijf, H.J.; Mendrik, A.M.; Biessels, G.J.; Pluim, J.P.W.; Išgum, I. Evaluation of a deep learning approach for the segmentation of brain tissues and white matter hyperintensities of presumed vascular origin in MRI. NeuroImage Clin. 2018, 17, 251–262. [CrossRef]

[12] MRBrainS: Evaluation Framework for MR Brain Image Segmentation. Availableonline: https:// mrbrains13 .isi.uu.nl /(accessed on 12 December 2020).

[13] Ronneberger, O.; Fischer, P.; Brox, T. U-Net: Convolutional Networks for Biomedical Image Segmentation. In Proceedings of the 18th International Conference on Medical Image Computing and Computer-Assisted Intervention—MICCAI, Munich, Germany, 5–9 October 2015; Navab, N., Hornegger, J., Wells, W., Frangi, A., Eds.; LNCS. Springer: Cham, Switzerland, 2015; Volume 9351, pp. 234–241.

[14] ISBI Challenge: Segmentation of Neuronal Structures in EM Stacks. Available online:http://brainiac2.mit.edu/isbi_challenge (accessed on 15 December 2020).

[15] Chaddad, A.; Tanougast, C. Quantitative evaluation of robust skull stripping and tumor detection applied to axial MR images. Brain Inf. 2016, 3, 53–61. [CrossRef] [PubMed]

[16] Lecun, Y.; Bottou, L.; Bengio, Y.; Haffner, P. Gradient-based learning applied to document recognition. Proc. IEEE 1998, 11, 2278–2324. [CrossRef]

[17] Shelhamer, E.; Long, J.; Darrell, T. Fully Convolutional networks for semantic segmentation. IEEE Trans. Pattern Anal. Mach. Intell. 2017, 39, 640–651. [CrossRef] [PubMed]

[18] Badrinarayanan, V.; Kendall, A.; Cipolla, R. SegNet: A deep convolutional encoder-decoder architecture for image segmentation. IEEE Trans. Pattern Anal. Mach. Intell. 2017, 39, 2481–2495. [CrossRef]

[19] Krizhevsky, A.; Sutskever, I.; Hinton, G.E. ImageNet classification with deep convolutional neural networks. Comms. ACM 2017, 60, 84–90. [CrossRef]

[20] Al-Antari, M.A.; Al-Masni, M.A.; Choi, M.-T.; Han, S.M.; Kim, T.-S. A fully integrated computer-aided diagnosis system for digital X-ray mammograms via deep learning detection, segmentation, and classification. Int. J. Med. Inform. 2018, 117, 44–54. [CrossRef]

[21] Mazurowski, M.A.; Buda, M.; Saha, A.; Bashir, M.R. Deep learning in radiology: An overview of the concepts and a survey of the state of the art with focus on MRI. J. Magn. Reson. Imaging 2019, 49, 939–954. [CrossRef]

[22] Chartrand, G.; Cheng, P.M.; Vorontsov, E.; Drozdzal, M.; Turcotte, S.; Christopher, J.P.; Kadoury, S.; Tang, A. Deep learning: A primer for radiologists. Radiographics 2017, 37, 2113–2131. [CrossRef]

[23] Mohsen, H.; El-Dahshan, E.-S.A.; El-Horbaty, E.-S.M.; Salem, A.-B.M. Classification using deep learning neural networks for brain tumors. Future Comput. Inform. J. 2018, 3, 68–71. [CrossRef]

[24] Manjula Devarakonda Venkata, Sumalatha Lingamgunta ,A Convolution Neural Network based MRI breast mass diagnosis using Zernike moments,MaterialsToday:Proceedings, https://doi.org/10.1016/j.matpr.2021.06.133

[25] Abiwinanda, N.; Hanif, M.; Hesaputra, S.T.; Handayani, A.; Mengko, T.R. Brain tumor classification using convolutional neural network. In Proceedings of the World Congress on Medical Physics and Biomedical Engineering, Prague, Czech Republic, 3–8 June 2018; Springer: Singapore, 2019; pp. 183–189.

[26] Pashaei, A.; Sajedi, H.; Jazayeri, N. Brain Tumor Classification via Convolutional Neural Network and Extreme Learning Machines. In Proceedings of the 8th International Conference on Computer and Knowledge Engineering (ICCKE), Mashhad, Iran, 25–26 October 2018; Curran Associates: New York, NY, USA, 2018; pp. 314–319.

[27] Sultan, H.H.; Salem, N.M.; Al-Atabany, W. Multi-classification of brain tumor images using deep neural network. IEEE Access 2019, 7, 69215–69225. [CrossRef]

[28] D Sirisha, S Sambhu Prasad, "MPEFT: A Makespan Minimizing Heuristic Scheduling Algorithm for Workflows in Heterogeneous Computing Systems", CCF Transactions on High Performance Computing. Aug. 2022. DOI: 10.1007/s42514-022-00116-w

[29] Sirisha, D. Complexity versus quality: a trade-off for scheduling workflows in heterogeneous computing environments. The Journal of Super Computing, 79, 924–946, (2023). DOI:10.1007/s11227-022-04687-x

[30] Manjula Devarakonda Venkata1, Sumalatha Lingamgunta& K Murali, Health Care Automation in Compliance to Industry 4.0 Standards: A Case Study of Liver Disease Prediction ,Journal of Scientific & Industrial Research , Vol. 82, February 2023, pp. 263-268, DOI: 10.56042/jsir.v82i2.70215

[31] Anaraki, A.K.; Ayati, M.; Kazemi, F. Magnetic resonance imaging-based brain tumor grades classification and grading via convolutional neural networks and genetic algorithms. Biocybern. Biomed. Eng. 2019, 39, 63–74. [CrossRef]

[32] Sirisha D., Prasad S.S. (2020), "A Relativistic Study on Recent Clustering Algorithms", In: Satapathy S.C., Bhateja V., Ramakrishna Murty M., GiaNhu N., JayasriKotti (eds) Communication Software and Networks, Lecture Notes in Networks and Systems, Vol. 134. Springer, Singapore. 04 October 2020,https://doi.org/10.1007/978-981-15-5397-4_19. ISSN 2367-3370